

## **Links between bismuth incorporation and surface reconstruction for GaAsBi growth probed by in situ measurements**

**C. Cornille,<sup>1,2, a)</sup> A. Arnoult,<sup>1</sup> Q. Gravelier,<sup>1</sup> C. Fontaine<sup>1, b)</sup>**

<sup>1</sup>LAAS-CNRS, Université de Toulouse, 7 avenue du Colonel Roche, 31400 Toulouse, France

<sup>2</sup>Université Toulouse III – Paul Sabatier, 118, route de Narbonne, 31043, Toulouse CEDEX 4, France

a) *Email: clara.cornille@laas.fr*

b) *Email: chantal.fontaine@laas.fr*

### **Abstract**

Bismuth incorporation and surface reconstruction have been studied simultaneously during GaAsBi growth by molecular beam epitaxy by means of in-situ wafer curvature monitoring and reflection high energy electron diffraction, respectively. Growth temperature and flux ratio have been varied successively. As/Ga atomic ratio close to the unity has been applied for the study of growth temperature effect. During the growth regime under the (1x3) reconstruction, Bi incorporation is found to be independent of the growth temperature, for temperatures where Bi desorption is insignificant. On the contrary, Bi incorporation becomes highly dependent on growth temperature as soon as the (2x1) reconstruction regime is reached. Only for the lower temperatures, the Bi incorporation gets to the same level during the (2x1) reconstruction than for the (1x3) reconstruction. When the As/Ga flux ratio is increased, bismuth

incorporation is observed to decrease for GaAsBi growth in the (2x1) reconstruction regime. Our results indicate that the (1x3) and (2x1) surface reconstructions are always successively observed, and that an energy barrier has to overcome to transit from the (1x3) to the (2x1) reconstruction, this mechanism being temperature dependent. Finally, a difference in surface stress with reconstruction has been identified.

## I. Introduction

GaAsBi alloys have attracted a great interest these last years since they exhibit peculiar properties which are highly promising for GaAs-based device applications in the fields of optoelectronics, photovoltaics and spintronics.<sup>1,2</sup> The large difference in the atomic properties of bismuth and the ones of the matrix constitutive elements, gallium and arsenic, is at the origin of these properties. First, the alloy bandgap strongly decreases when bismuth content increases, of the order of 83meV/%Bi for low Bi contents.<sup>3</sup> Bismuth, acting as an iso-doping element, mainly perturbs the GaAs valence band forming Bi aggregates and alloy disorder. This results into carrier localization, and leads to a significant increase of the spin-orbit split-off energy which could help reduce Auger losses.<sup>2</sup> High quality alloys can be grown using molecular beam epitaxy (MBE)<sup>4,5</sup> and metalorganic vapor phase epitaxy.<sup>6,7</sup>

The MBE growth of these emerging highly mismatched alloys has been shown to be subtle as the control of bismuth incorporation is challenging. Indeed, it highly depends on growth conditions. Numerous publications have alerted on the need in the case of MBE to employ atomic V/III ratios close to the unity irrespective of the species used for arsenic: As<sub>4</sub> obtained by As sublimation<sup>4</sup> or As<sub>2</sub> created by As<sub>4</sub> thermal

cracking.<sup>5</sup> This ratio refers to atomic adsorbed V (As and Bi) and III (Ga) atomic species population. If too high V/III ratios are used, the material quality is altered and incorporation decreases.<sup>8</sup> The main drawback of GaAsBi growths carried out under such a unity V/III ratio is the risk to form droplets, consisting of Ga. Sometimes Bi droplets are also observed too<sup>9,10</sup> which indicates incomplete incorporation of Bi species. As for the substrate temperature, its major role has been reported to be the increase in achievable bismuth alloy content with decreasing growth temperature.<sup>8</sup> However higher temperatures yield better alloy quality.<sup>11</sup> Moreover low growth temperature has been claimed to promote the growing GaAsBi to exhibit a CuPt ordering in the (2x1) growth regime.<sup>12</sup> Finally, large Bi clusters can even be formed in these alloys grown at very low temperatures and subsequently annealed, pointing out some metastability.<sup>13,14</sup> The role of surface reconstruction has also been shown to be major, the (2x1) reconstruction has been reported to lead to a more efficient Bi incorporation.<sup>8</sup> Nevertheless, all these mechanisms are still being under study in order to form a comprehensive understanding of GaAsBi growth with a view to master the growth of high quality GaAsBi alloys with high bismuth concentrations as required for the targeted and above-mentioned applications.

Here we investigate the growth of GaAsBi on (001) GaAs by MBE using wafer curvature measurements and reflection high energy electron diffraction analysis (RHEED). The simultaneous use of these techniques has allowed us to get information on the effect of the growth temperature and As/Ga atomic ratio on Bi incorporation. We have found that Bi incorporation is linked to the surface reconstruction during GaAsBi growth.

## II. EXPERIMENT

### A. Growth

GaAsBi layers have been grown on (001) undoped 50mm-diameter GaAs wafers in a 412 RIBER MBE system. 350 $\mu$ m-thick wafers were used all samples. This R&D system provides vertical growth geometry: the substrate is not clamped but placed free on its substrate-holder, and twelve cells are available, containing Ga, As (cracker), Bi, Al, ... elements, with excellent uniformity flux distribution (1%) over the wafer surface thanks to the substrate rotation around its axis at about 12rpm. This system is equipped with a home-made in-situ optical monitoring of the wafer curvature inferring the curvature from the measurement of the magnification of a virtual image, which allows real-time monitoring of the GaAsBi growth while the substrate is rotating.<sup>15</sup> Recording of the RHEED patterns is also carried out and light scattering is used to control droplet formation at the growing surfaces. Before the start of the growths, careful measurements of each flux (beam equivalent pressure (BEP)) are performed thanks to a Bayard-Alpert gauge. The Ga flux was selected such a way that the GaAs growth rate is 0.3 micrometer/hour ( $\mu$ m/h) and the Bi flux selected to be sufficiently low to be sure that no Bi droplets were formed; The Bi cell temperature was equal to 439°C for sample A and C, and 433°C for sample B. These samples belong to different series. The As<sub>4</sub> flux, emitted from the As cell without being cracked, was adjusted so as to provide a ratio slightly higher than unity (1.05 ( $\pm$ 5%)) for the adsorbed As and Ga atomic species on the GaAs surface, by using the procedure provided by Newstead et al..<sup>16</sup> We will use the As/Ga atomic ratio as a parameter in this study, rather than BEP ratio, since it is more meaningful. Substrate temperature is measured by thermometry (kSA BandiT) with the

values available in the kSA BandIT software for similar substrates. The measured values were compared for the deoxidation temperature of an epi-ready GaAs substrate and for the temperature leading to the change from the static (2x4) reconstruction to the (c(4x4) reconstruction<sup>17</sup>. The precision on the temperatures is estimated to be in the 2-3% range. The GaAsBi layers under study were grown with As<sub>4</sub>; Ga and Bi shutters were simultaneously opened at the start of their growth.<sup>18</sup>

For all the samples, a 300nm-thick GaAs buffer layer was grown at 580°C before ramping down the wafer temperature to perform GaAsBi growth. At each change of growth temperature care was taken to stabilize its value. The first sample (sample A) grown consists in a GaAsBi layer grown at 280°C and at a As/Ga ratio close to the unity. Wafer curvature and RHEED measurements were carried out along its growth. At the end of its growth, the substrate temperature was quenched. This sample was then withdrawn from the MBE system, and its surface was studied by optical microscopy and atomic force microscopy in order to check the possible presence of droplets. The Bi fraction of the layer was inferred from curvature evolution during growth of the GaAsBi layer and also measured by High Resolution X-ray Diffraction (HR-XRD), in order to compare the results and validate the curvature measurements.

The two other samples (B and C) consist of a multilayer formed by 30nm-thick GaAsBi (except for the last one, 80nm thick) grown at low temperature and 50nm-thick intermediate GaAs layers. The first 5nm of these GaAs spacers were systematically grown at the same low temperature as GaAsBi in order to cap the alloy surface; this prevents the surface from any roughening during the increase of substrate temperature for the growth of the remaining GaAs spacers at 580°C.

<b>Sample</b>	<b>Growth rate (<math>\mu\text{m/h}</math>)</b>	<b>Layer thickness (nm)</b>	<b>As/Ga</b>	<b>Growth temperature (<math>^{\circ}\text{C}</math>)</b>
<b>A</b>	<b>0.3</b>	<b>85</b>	<b>1.05</b>	<b>280</b>
<b>B (multilayer)</b>	<b>0.3</b>	<b>30 (80)</b>	<b>1.05</b>	<b>422 to 273 (265)</b>
<b>C (multilayer)</b>	<b>0.3</b>	<b>30</b>	<b>1.05 to 8</b>	<b>280</b>

Table 1. Details on growth conditions used for the GaAsBi layers in the grown samples: GaAs growth rate calibrated by XRD, layer thickness(es), As/Ga atomic ratio, and growth temperature(s) measured by thermometry (kSA BandiT).

For sample B, the As/Ga atomic ratio was still kept about equal to the unity, whereas the growth temperature was varied to provide information on its influence on sample curvature, and thereby on Bi incorporation along GaAsBi growth. For sample C, the substrate temperature was kept constant and the  $\text{As}_4$  flux was varied in order to yield As/Ga atomic ratios in the 1-8 range and study its influence on Bi incorporation. The growth of these samples therefore provides information on the influence of these two key parameters on GaAsBi growth.

Details on the three samples used in this study are given in Table 1. Note that the thicknesses indicated for the GaAsBi layers do not correspond to their exact layer thicknesses, but to the equivalent GaAs thicknesses calculated as the product of the GaAs growth rate by the GaAsBi growth duration from the opening of the Ga and Bi cell shutters.

## B. Wafer curvature, layer strain and Bi incorporation

Optical curvature measurements allow us to get insight into the stress within growing pseudomorphic strained layers. The wafer curvature ( $\kappa$ ) generated by growth of a strained layer can be calculated using the Stoney equation as:<sup>18</sup>

$$\kappa = \frac{1}{R} = \frac{6\sigma h_f}{M_s h_s^2} \quad (1)$$

where  $R$  is the wafer curvature radius,  $\sigma$  is the stress in the growing film,  $h_f$  and  $h_s$  are its thickness and the substrate thickness respectively, and  $M_s$  is the bulk modulus of the substrate calculated from the GaAs  $C_{ij}$  coefficients.<sup>20</sup> It is equal to 123.87 GPa. Note that the wafer curvature is dependent on the thickness and bulk modulus of the substrate. On the contrary,  $\sigma \cdot h_f$  that we will call in the following “stress.thickness” is independent of these values, is given as GPa.nm, or N/m, and is therefore homogeneous to a surface energy density. For this reason it is often used as a variable<sup>21</sup> and will be indicated in the figures of this paper, together with the wafer curvature.

The biaxial stress ( $\sigma$ ) supported by a pseudomorphically strained layer grown is constant; it corresponds to the slope of the stress.thickness as a function of the increasing film thickness. This stress is related to the in-plane layer elastic strain ( $\varepsilon$ ) due to lattice parameter misfit:

$$\varepsilon_f = \frac{\sigma}{M_f} \quad (2)$$

where  $M_f$  is the bulk modulus of the material constituting the film, here the GaAsBi alloy. We have taken  $M_f$  equal to the bulk modulus of the GaAs substrate ( $M_s$ ).

The Bi content of a pseudomorphically strained GaAsBi layer ( $x_{Bi}$ ) is related to its strain:

$$x_{Bi} = -\varepsilon_f \frac{a_{GaAs}}{a_{GaBi} - a_{GaAs}} \quad (3)$$

where  $a_{\text{GaAs}}$  and  $a_{\text{GaBi}}$  are the GaAs and GaBi lattice parameters at growth temperature. Calculation is done in this paper with their room temperatures values, 5.6534 Å and 6.33 Å respectively,<sup>22</sup> since we have considered that the thermal coefficients for both materials are the same. We have then done two approximations on these operands which need to be refined in the future.

The Bi content of a pseudomorphically strained GaAsBi layer ( $x_{\text{Bi}}$ ) can so be calculated from curvature measurements using these equations.

It is important to emphasize that curvature of the wafer would change if any additional event adding or lowering stress in the wafer occurs. i) An external force exerted on the wafer; in our case, the substrate is placed horizontally top-down on the molybdenum support without any clamp to prevent any mechanical stress from occurring. ii) Temperature difference between surface and back side of the sample,<sup>23</sup> to get rid of this detrimental effect in our analysis, we have paid attention to reset at zero the curvature for each GaAsBi growth after sample temperature stabilization. iii) Surface stress, due for instance to a surface reconstruction; in that case, the additional curvature would be constant along growth and, in the case of a pseudomorphic growth, would not affect the slope of the curvature evolution used for calculation of the layer composition. iv) Generation of defects in a high density; for instance the formation of misfit dislocations which release layer stress will lead to damping wafer curvature variation.

Curvature measurements have been already used to measure the strain relaxation which occurs in thick dilute bismide layers.<sup>24</sup> For GaAsBi layers with small thickness and low bismuth content such as the ones under study, no significant plastic stress relaxation has been found; the GaAsBi layers are pseudomorphically strained on their GaAs substrate. So stress can here be used to estimate their in-plane elastic strain and,



thereby, their Bi fraction. Moreover, it was shown that GaAsBi composition ( $x_{\text{Bi}}$ ) estimated from curvature measurements is in agreement with the values inferred from XRD analysis.<sup>25</sup>

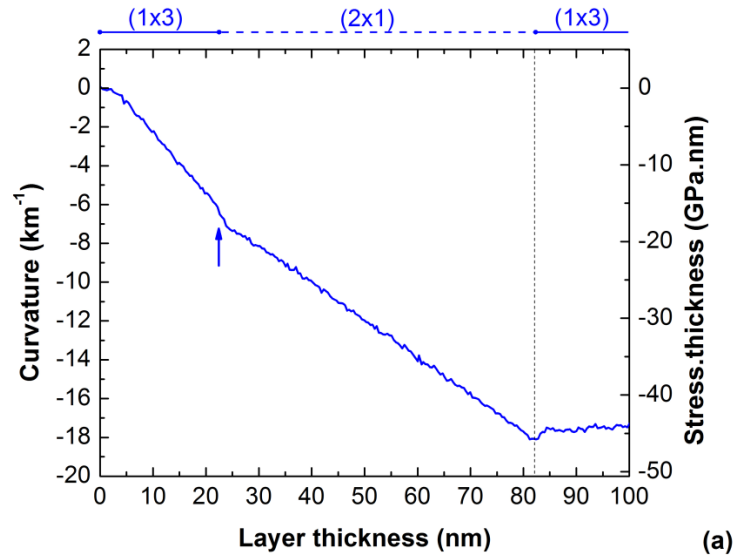
In order to get this comparison, HR-XRD was performed on sample A using a D8 Discover Bruker equipment in order to determine, from  $\omega/2\theta$  transverse scans, its bismuth composition profile. To extract the thickness and alloy composition of the grown layer by using the Bruker Leptos software, the same material constants as for the treatment of the curvature measurements, indicated above, have been used.

### **III. RESULTS AND DISCUSSION**

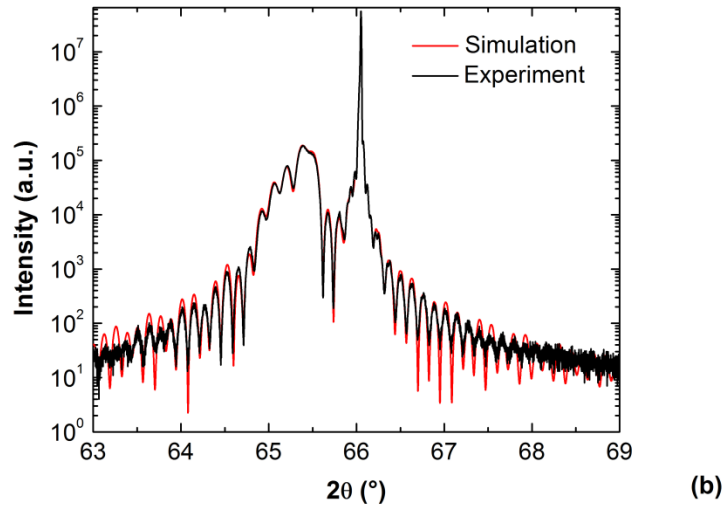
#### **A. Curvature and surface reconstruction along the growth of a single GaAsBi layer**

Fig.1 shows the evolution of curvature along GaAsBi growth for sample A. We observe that the curvature is negative and that its value increases as far as the layer is thickening, as expected for growth of a compressively strained layer.

Upon opening of the Ga and Bi shutters, the recorded RHEED pattern shows that the surface reconstruction changes immediately from the  $c(4\times 4)$  low temperature GaAs surface reconstruction to the  $(1\times 3)$  GaAsBi one, and that the curvature remains small up to a 4.5nm equivalent GaAs thickness for all the investigated temperatures. This could be associated to a delay for efficient Bi incorporation observed in the case of these highly mismatched alloys grown by MBE<sup>26</sup> and MOVPE<sup>7</sup> and often attributed to Bi segregation. Such a segregation effect has already been observed for other elements, like indium<sup>27</sup> and antimony.<sup>28</sup> It is related with element segregation up to a certain atomic population needed for its steady-state incorporation. It can be avoided by anticipating



(a)



(b)

FIG. 1. (a) Wafer curvature and surface reconstructions evolution along growth of sample A; (b) its HR-XRD diffractogram. Note that the Ga and Bi cell shutters were opened and closed together when the layer thicknesses were respectively equal to 0 and 85nm.

this mechanism, by starting Bi deposit before opening the Ga cell shutter, like it is done by some groups working on dilute bismides.<sup>7,11</sup> Here, we do not prevent it from occurring.<sup>18</sup>

Then as growth of the layer proceeds, the curvature starts to evolve linearly, indicating steady-state Bi incorporation into GaAs. The (1x3) surface reconstruction is preserved at first, before changing to the (2x1) one. This change in reconstruction observed by RHEED has also a signature on the curvature variation: this transition is systematically associated with a step in the curvature, as observed in Fig. 1 (see the arrow). This step starts upon the apparition of the (2x1) reconstruction RHEED pattern. This peculiar result will be discussed later. Then growth proceeds in the (2x1) reconstruction regime. As can be observed, the curvature evolution is weaker after the reconstruction change, which should indicate that the stress is smaller during the GaAsBi growth on the (2x1) reconstructed surface than on the (1x3) reconstructed one, and therefore that the Bi content in the growing GaAsBi has become lower.

Once sample A was withdrawn from the growth chamber, the observation of its surface by optical microscopy did not show the presence of any droplet, neither its observation by atomic force microscopy. So we conclude that the Bi atomic excess desorbs from the surface in spite of the low temperature used for the growth of this sample. This will be discussed later.

The simulation of the ex-situ HR-XRD diffractogram indicates that sample A contains a GaAsBi layer which exhibits two Bi fractions. Table 2 shows these values, compared with the values of the Bi fractions ( $x_{\text{Bi}}$ ) and sublayer thicknesses inferred from the evolution of the curvature during its growth. These are in a quite good agreement. Only slight discrepancies can be observed; these can be related to the approximations

	Interfacial sublayer (1)		Uppermost sublayer (2)	
<b>Analysis technique</b>	<b>Thickness (nm)</b>	<b>Atomic fraction (%)</b>	<b>Thickness (nm)</b>	<b>Atomic fraction (%)</b>
<b>In situ curvature</b>	<b>21</b>	<b>5.55</b>	<b>61</b>	<b>3.30</b>
<b>Ex situ X-ray Diffraction</b>	<b>24.7</b>	<b>5.63</b>	<b>57.4</b>	<b>3.63</b>

Table 2. Comparison between the thickness and Bi fraction of the two GaAsBi sublayers in sample A measured by in situ curvature and ex-situ HR-XRD analysis techniques.

done on the operants used for calculation (equality of their values at high and room temperature). Further work is needed to check their eventual different dependence on temperature and understand the origin of the observed discrepancies. Nevertheless, both characterization techniques demonstrate the presence of two different Bi fractions within the layer, higher close to the interface and lower close to the surface. These HR-XRD measurements confirm that the change in reconstruction has led to lower the Bi incorporation during growth and that in-situ curvature measurements provides information on Bi incorporation into the growing layer.

### **B. Effect of growth temperature on Bi incorporation and surface reconstruction**

Fig.2 shows the curvature evolution along GaAsBi growth for sample B. In this sample, GaAsBi layers were successively grown at different growth temperatures. In

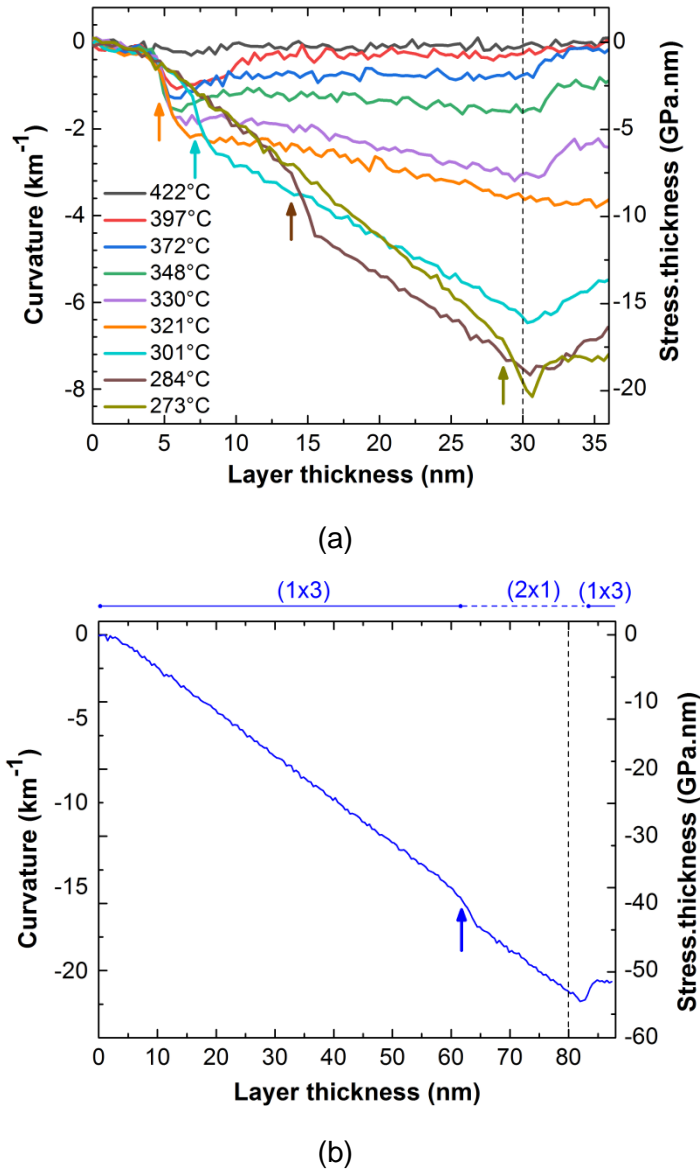


FIG..2. Curvature along growth measured for the successive GaAsBi layers during their growth: (a) at different growth temperatures between 422°C and 273°C, and (b) at 265°C. The Ga and Bi cell shutters were opened together (0nm); the Bi cell shutter was closed for the successive growths when the layer thickness is 30nm, except for the last one at 265°C: 80nm. The arrows indicate the change in surface reconstruction, from (1x3) to (2x1), observed by RHEED during GaAsBi growth. In the upper part of Fig.2.(b), are shown the different surface reconstructions observed along growth. Note that the curvature and thickness are reset at zero at the start of each GaAsBi growth.

order to ease the comparison in the curvature evolution for each layer, thickness and curvature are reset at zero in Fig.2.

We observe the same features in the curvature variation and surface reconstruction change as for sample A: the direct change from the  $c(4\times 4)$  reconstruction to the  $(1\times 3)$  one upon opening of Ga and Bi cell shutters; at first, a small curvature variation indicating a transient towards the steady-state Bi incorporation, where the curvature variation is more pronounced; the change from the  $(1\times 3)$  reconstruction to the  $(2\times 1)$  one; a smaller slope (stress) after this reconstruction change, except for the last layer grown at the lower temperature (Fig. 2. b) where the slope is the same for both reconstructions; and finally a recovery of the  $(1\times 3)$  reconstruction at the closing of the Bi cell shutter. As for sample A also, the  $(1\times 3)/(2\times 1)$  transition – during GaAsBi growth and at its end - is systematically associated with a step in the curvature, whatever the growth temperature, as observed in Fig. 1. This step starts upon the apparition of the  $(2\times 1)$  reconstruction RHEED pattern during growth and ends when the  $(1\times 3)$  reconstruction is observed at the end of the GaAsBi growth. This peculiar result will be discussed later.

The decrease in growth temperature is observed to have other significant effects on the GaAsBi growing layer. For the four higher temperatures investigated, from  $422^{\circ}\text{C}$ , down to  $348^{\circ}\text{C}$ , the  $(1\times 3)/(2\times 1)$  surface reconstruction change is about immediate. However, the  $(2\times 1)$  reconstruction is not maintained for the two highest temperatures. It can be identified in Fig.2 a by steep curvature changes (“steps”), at its appearance and disparition. The  $(1\times 3)$  reconstruction is observed to be recovered after a growth of about some nm ( $\sim 1\text{-}5\text{nm}$ ) equivalent GaAs thickness. Simultaneously the curvature is observed to decrease again to a weak value closer to zero for the highest temperature and then to remain about constant. This indicates that Bi incorporation is

insignificant, the Bi species adsorbed onto the surface, additional to the ones involved into the reconstruction, being desorbed before their incorporation. The fact that the (2x1) reconstruction appears in a transient way could be accounted for by some surface reconstruction instability of this Bi-rich GaAs surface for this high range of growth temperature subjected to Bi desorption, or due to Bi transient upon Bi shutter opening. At the two next growth temperatures, 372°C and 348°C, a slight residual curvature is observed; its value is constant along the layer growth and larger for 348°C. This can originate from the signature of a mixed character for the reconstruction which could be locally of the (2x1)-type and become (2x1)-richer as the temperature decreases, but is not related to any significant Bi incorporation. The continuation of the (2x1) reconstruction up to the end of the layer growth is confirmed by the final curvature step when the Bi cell shutter is closed.

For the lower growth temperatures ( $T < 348^\circ\text{C}$ ), the (1x3) reconstruction is found to last longer (see arrows in Fig. 2) before its transition to the (2x1) reconstruction. During the (1x3) regime, the curvature evolution is the same for all the layers, even if grown at different temperatures. By contrast, the curvature value changes with growth temperature in the (2x1) regime; its value is observed to increase when temperature drops. Then, when the Bi cell shutter is closed to stop the alloy growth, the curvature value is observed to stabilize and then decrease until the (1x3) reconstruction is completely recovered. During the subsequent 5nm low temperature growth, the (1x3) Bi-rich reconstruction is still maintained. However, since the (1x3) reconstruction is no longer enriched with the Bi impinging species, a GaAs layer is formed. During its growth, the curvature is observed not to evolve any longer: it means this layer is unstrained, which indicates that the underlying GaAsBi layer was completely elastically strained at

the end of its growth otherwise the plastic relaxation induced by dislocation generation would have occurred within GaAsBi and the subsequently grown GaAs layer would have supported an in-plane tensile stress, leading to a positive slope of the curve, which it is not the case.

Let us come back to the two steep curvature changes observed during the GaAsBi growth in its (2x1) reconstruction regime in Fig. 1 and Fig. 2. These are reproducible in this study whatever the growth temperature. It is worth noting that they have also been observed in most GaAsBi/GaAs growths that we have carried out. We propose that these steep curvature changes be related to a change in surface stress between these two observed reconstructions. Indeed, this contribution to the curvature is constant during the entire GaAsBi growth in the (2x1) reconstruction regime and stops when the (1x3) reconstruction is observed again. Surface elastic strain at Bi sites was already evoked in the literature to account for Bi-rich reconstructions<sup>29</sup> since Bi atoms are much larger than the Ga and As atoms. The (2x1) reconstruction has been shown to be Bi-richer than the (1x3) one and is saturated with Bi-Bi bondings.<sup>30</sup> The (2x1) reconstruction could therefore exhibit a surface stress different from the (1x3) reconstruction.

We show the Bi content evolution in the growing layer with growth temperatures for the two reconstructions in Fig. 3. Note that we could not measure the Bi fraction for the GaAsBi layers grown at wafer temperatures higher than 321°C in the (1x3) regime since the (1x3)/(2x1) transition was quasi instantaneous at the start of the growth. The Bi fraction of the GaAsBi layers grown under the (1x3) reconstruction regime from 300°C to 265°C is calculated from the curvature measurements to be equal to 4.6 %



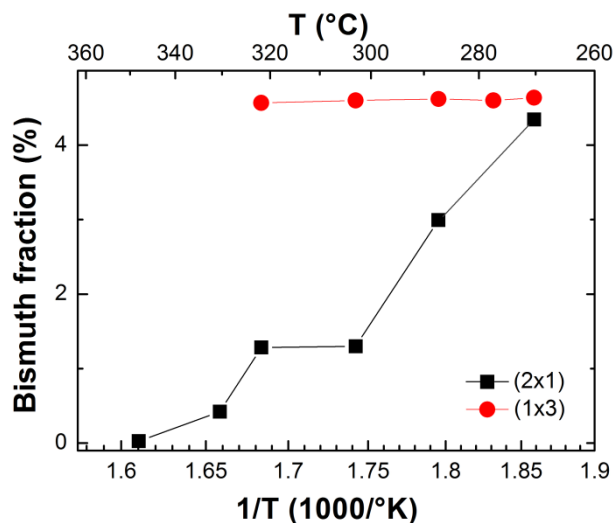


FIG. 3. Variation of the Bi fraction ( $x_{\text{Bi}}$ ) in the layer with growth temperature ( $T_g$ ).  $x_{\text{Bi}}$  has been inferred from the wafer curvature measurements performed during GaAsBi growth on (1x3) (red circles) and (2x1) (black squares) reconstructed surfaces.

whatever the temperature. The Bi content for the GaAsBi material grown under the (2x1) regime increases when the growth temperature decreases up to the value found in the (1x3) regime.

Once the (1x3) regime is steady-state (i.e. after 4.5nm grown), Bi incorporation is effective for growth temperatures less than 350°C, and is found to remain the same whatever the growth temperature is. Since Bi composition does not depend on the growth temperature, it means that all the Bi species adsorbed at the surface are efficiently incorporated into the material grown, forming a GaAsBi alloy with a constant Bi concentration, whatever the growth temperature. In this temperature range, the Bi desorption rate from a (1x3) reconstructed GaAs<sup>31</sup> is not significant. It is worth noting that this does not mean that all the Bi species of the flux impinging from the Bi cell play a role in Bi surface diffusion and incorporation mechanisms. Indeed, the Bi sticking

coefficient can be smaller than the unity. This is possible since this Bi element flux was found also to involve  $\text{Bi}_2$  molecular species.<sup>32</sup>

By contrast, we observe from the curvature variation in Fig. 3 that the Bi incorporation is highly dependent on the growth temperature, for the part of GaAsBi growth done in the (2x1) reconstruction regime. When the bismuth content in the part of the GaAsBi layers grown with the (2x1) reconstruction is smaller than in the (1x3) regime, despite the low growth temperature range used. Previous literature on GaAsBi grown by MBE with  $\text{As}_4$  or  $\text{As}_2$  claims that the incorporation is higher when growth is performed in the (2x1) reconstruction regime.<sup>8</sup> This discrepancy with our present results can be accounted for by the fact that the earlier studies were using higher growth temperature to get the (1x3) reconstruction regime where the (1x3)/(2x1) transition is about instantaneous at such low As/Ga ratio. Note that, in our experiments, the (1x3) regime is only temporary and then changes to the (2x1) reconstruction; to our knowledge, such a result for GaAsBi growth has not been observed yet. The presence of two Bi contents within GaAsBi layers, with a higher Bi content at the start of the growth, has already been published,<sup>33,34</sup> change in the alloy composition was attributed to CuPt ordering in the first grown alloy which would promote Bi incorporation, and/or to unsuitable growth conditions. We show here that, for GaAsBi growth with a V/III atomic ratio close to the unity, the use of too high growth temperature leads to such a result and that sufficiently decreasing substrate temperature leads to equalize the Bi incorporation for both reconstructions.

Since the impinging Bi flux is constant, and that the Bi fraction is higher for the layer grown in the (1x3) reconstruction regime, the question raises from this study on the mechanism which eliminates the excess of bismuth from the growing surface in the

(2x1) reconstruction regime. Bismuth droplets can be formed and/or desorption of the Bi atomic excess can be activated. We did not observe by diffuse light scattering any feature during the growth indicating Bi droplets would have been formed, neither by atomic force microscopy on the surface of sample A. In that case, it means that Bi desorption is enhanced on the (2x1) reconstructed surface compared to the (1x3) reconstructed surface; this mechanism could originate from the difference in Bi surface bonding nature and population of Bi species of the two reconstructions.<sup>31</sup> The (2x1) reconstructed surface is about completely saturated by bismuth. The desorption rate of the bismuth could in such conditions become significant, much higher than on a (1x3) reconstructed surfaces only partially covered by bismuth. Note that GaAsBi growth goes on after closing the Bi cell shutter. This unexpected incorporation ends as soon as the reconstruction is observed by RHEED to transit towards the (1x3) reconstruction. Since we do not observe any droplet, this can origin from the Bi atoms involved in the (2x1) reconstruction, in excess relative to the (1x3) reconstruction, that incorporate as growth proceeds up to the formation of the (1x3) reconstruction.

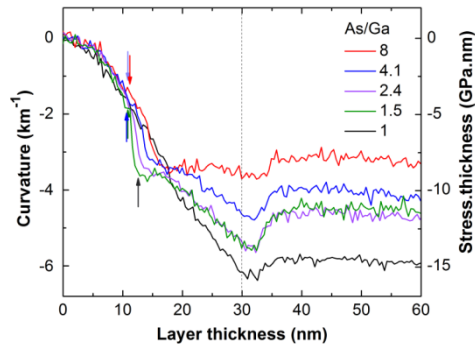
The last relevant information to be drawn from this part of study is the fact that the transition between the two surface reconstructions is observed to be highly dependent on growth temperature. As observed in Fig. 2, this (1x3)/(2x1) transition appears later when temperature gets lower. This mechanism is thus thermally activated, even if this evolution does not perfectly fit a simple Arrhenius dependence. We propose that an energy barrier exists upon reconstruction change due to the need for the Bi atoms involved in the (1x3) reconstruction to bond differently to get the (2x1) reconstruction.

### **C. Effect of the arsenic overpressure in Bi incorporation**

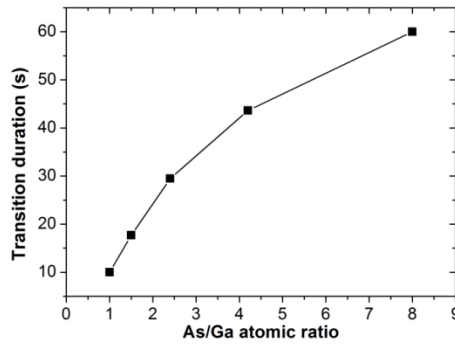
In order to get an insight into the effect of an As overpressure and thereby further improve understanding of the surface mechanisms involved in Bi incorporation at the surface of a growing GaAsBi layer, the As<sub>4</sub> beam equivalent pressure (BEP) was increased while the Ga and Bi BEPs as well as the growth temperature (280°C) were kept constant. So the As/Ga ratio and the As/(As+Bi) ratio were both changed. We again use the As/Ga atomic ratio as a parameter in this study. This ratio was varied in sample C, successively, selected equal to 1, 1.5, 2.4, 4.2 and 8. As for sample B, we have reset at zero the curvature and thickness for each successive GaAsBi layers in order to get easier comparison. Fig. 4 (a) depicts these variations.

Compared to the other samples, the change in the As/Ga ratio doesn't change the nature of the features along growth after simultaneous opening Bi and Ga cell shutters: i) the curvature variation is small at the start of the growth; ii) it becomes more pronounced during GaAsBi growth in the steady-state (1x3) reconstruction regime; iii) the transition occurs; iv) the surface is (2x1) reconstructed during the rest of the growth; v) after closing of the Bi cell shutter, the surface reconstruction changes to the (1x3) one.

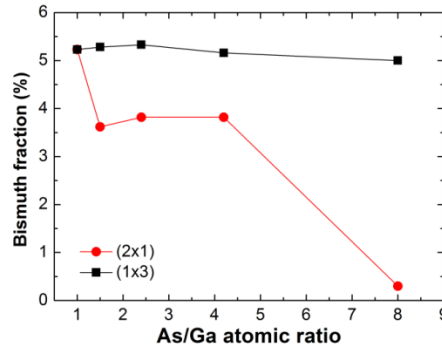
Again also Fig. 4 (b) shows that there is a great difference in Bi incorporation according to the type of surface reconstruction. While Bi incorporation is only slightly affected by the As/Ga ratio increase when growth proceeds in the (1x3) surface reconstruction regime, it is dramatically reduced in the (2x1) reconstruction growth regime. In the intermediate As/Ga range, it does not evolve a lot but is weaker than when a As/Ga unity ratio is used. However, when the As/Ga is equal to 8, Bi incorporation is about equal to zero.



(a)



(b)



(c)

FIG.4. (a) Wafer curvature evolution for the successive GaAsBi layers measured during their growth at different As/Ga atomic ratios and at a growth temperature equal to 280°C (simultaneous opening of the Ga and Bi cell shutters); (dashed vertical line) closing of the Bi cell shutter. The arrows indicate the change in surface reconstruction from (1x3) to (2x1) observed by RHEED; (b) GaAsBi layer grown during the (1x3)/(2x1) transition (curvature change duration); (c) variation of the Bi fraction ( $x_{\text{Bi}}$ ) of the GaAsBi growing layers on the (1x3) and (2x1) reconstructed surfaces inferred from the curvature measurement as a function of the As/Ga ratio.

Finally, the other great influence of the Arsenic overpressure on GaAsBi is observed on the surface reconstruction features. It affects the duration of the transition between the (1x3) and (2x1) reconstructions, which is again detected from the associated steep curvature change. For all the As/Ga ratios, the (2x1) RHEED pattern instantaneously appears upon the occurrence of the-curvature change. This reconstruction transition outset occurs at about the same moment for all the layers; no great difference is observed for this critical point, except when the the As/Ga ratio is equal to the unity which is not understood yet.

In Fig. 4 (a) the evolution of the curvature is expressed as a function of the grown thickness since the curvature due to pseudomorphic strain depends on this parameter (see equation 1). However, a reconstruction change involves surface mechanisms. So time would be also a more suitable variable to be used for the study of the surface transition. We get it directly during curvature measurements. Fig. 4 (b) shows the transition duration change when the As/Ga ratio increases. It is found to increase significantly as the As overpressure increases. It shows that the exchange mechanisms between the V species, As and Bi, during the incorporation mechanisms play a major role. Bi incorporation is carried out in close competition with As incorporation to the expected benefit of the As species, one of the main constituent of the matrix. This therefore plays a part in the relative incorporation of these two V species, particularly when the surface is already saturated with arsenic. As a result, these mechanisms increase Bi surface diffusion length and, as shown in this study, contribute to increase its desorption from this surface. Moreover, we show that it also becomes more difficult for the Bi species to succeed in forming the (2x1) reconstruction. These results confirm the

results of literature that already showed, thanks to ex-situ characterization techniques, that Bi incorporation decreases when the As overpressure is increased, whatever  $\text{As}_4$ <sup>32</sup> or  $\text{As}_2$ <sup>5</sup> are used. The use of a low As flux, of the order of the unity, is therefore mandatory to guarantee an efficient Bi incorporation.

#### **IV. CONCLUSIONS**

We have investigated bismuth incorporation and surface reconstruction via wafer curvature and RHEED measurements performed during GaAsBi growth, respectively. In this study, we have used a growth rate ( $0.3\mu\text{m/h}$ ), an As/III ratio close to the unity, and a low Bi flux. Here, we have studied the effect of growth temperature and of As overpressure on these properties. First, we have shown that the two reconstructions, (1x3) and (2x1), appear successively. We have found that different Bi incorporation regimes exist according to these surface reconstructions. First GaAsBi growth proceeds in the (1x3) reconstruction and Bi incorporation is observed to be complete as soon as its steady-state regime is established, and as growth temperature is low enough for the Bi desorption to be insignificant. On the contrary, Bi incorporation during alloy growth in the (2x1) growth regime, which is formed in a second step, strongly depends on the growth temperature. It increases as the growth temperature decreases; in our opinion this result originates from the almost complete Bi coverage of the (2x1) reconstructed surface, which significantly hinders its incorporation. The surface reconstruction providing the more efficient Bi incorporation, and therefore the higher Bi contents for the GaAsBi layers grown on GaAs, is identified as the (1x3) reconstruction. Finally the transition between these two Bi-rich reconstructions has been found to be associated with a thermally activated mechanism. This change in surface reconstruction is expected

to result in lowering surface stress,<sup>29,30</sup> but involves a great change in the Bi bonding at the surface. In our opinion, this mechanism is thermally-activated, because of the existence of an energy barrier associated with this Bi surface bonding re-arrangement. Upon this reconstruction transition, change in the curvature of the growing layer has been observed, the origin of which still remains to be understood. We propose that it is related with a difference in surface stress between these two Bi-rich reconstructed surfaces in the growth conditions used in this study. Finally, accordingly to literature, we confirm that the use of an arsenic overpressure decreases the Bi incorporation, and we show that this effect is much more significant when growth is performed in the (2x1) reconstruction regime. Moreover, we observe that the transition between the two reconstructions is also made more difficult when high As/Ga ratios are used but starts at the same layer thickness. This shows the major role of the exchange mechanisms of the V species in the Bi incorporation mechanism and confirms the need to use low V/III ratios, of the order of the unity, as already established.<sup>3-8</sup>

We plan now to take benefit from the coupling of the curvature and RHEED measurements to study the influence on Bi incorporation of the other growth parameters, growth rate and bismuth flux, and of their interplay. We have shown here that the results obtained with this coupling of in-situ techniques actually provide a complementary insight into molecular beam epitaxy of these peculiar alloys to the results already published. They show that more intense work is still needed to finely understand all the mechanisms which govern growth of GaAsBi by MBE.



## REFERENCES

- <sup>1</sup>T. Thomas, A. Mellor, N. P. Hylton, M. Führer, D. Alonso-Álvarez, A Braun, N. J. Ekins-Daukes, J. P. R. David and S J Sweeney, *Semiconductor Science and Technology* **30**, 1–6 (2015).
- <sup>2</sup>C. A. Broderick, S. Mazzucato, H. Carrère, T. Amand, H. Makhloufi, A. Arnoult, C. Fontaine, O. Donmez, A. Erol, M. Usman, E. P. O'Reilly, and X. Marie, *Physical Review B* **90**, 195301 (2014).
- <sup>3</sup>B. Fluegel, S. Francoeur, A. Mascarenhas, S. Tixier, E. C. Young, and T. Tiedje, *Physical Review Letters* **97**, 067205 (2006).
- <sup>4</sup>M. Yoshimoto, S. Murata, A. Chayahara, Y. Horino, J. Saraie, and K. Oe, *Japanese Journal of Applied Physics* **42**, L 1235 (2003).
- <sup>5</sup>R. B. Lewis, M. Masnadi-Shirazi, and T. Tiedje, *Appl. Phys. Lett.* **101**, 082112 (2012).
- <sup>6</sup>K. Oe and H. Okamoto, *Japanese Journal of Applied Physics* **37**, L1283 (1998).
- <sup>7</sup>P. Ludewig, Z.L. Bushell, L. Nattermann, N. Knaub, W. Stolz, and K. Volz, *Journal of Crystal Growth* **396**, 95 (2014).
- <sup>8</sup>M. Masnadi-Shirazi, D.A. Beaton, R.B. Lewis, X. Lu, and T. Tiedje, *Journal of Crystal Growth* **338**, 80 (2012).
- <sup>9</sup>G. Vardar, S. W. Paleg, M.V. Warren, M. Kang, S. Jeon, and R. S. Goldman, *Applied Physics Letters* **102**, 042106 (2013).
- <sup>10</sup>J. A. Steele, R. A. Lewis, J. Horvat, M. J. B. Nancarrow, M. Henini, D. Fan, Y. I. Mazur, M. Schmidbauer, M. E. Ware, S.-Q. Yu, and G. J. Salamo, *Scientific Reports* **6**, 28860 (2016).

- <sup>11</sup>T. B. O. Rockett, R. D. Richards, Y. Gu, F. Harun, Y. Liu, Z. Zhou, J. P. R. David, *Journal of Crystal Growth* **477**, 139 (2017).
- <sup>12</sup>D.F. Reyes, F. Bastiman, C.J. Hunter, D.L. Sales, A.M. Sanchez, J.P.R. David, and D. González, *Nanoscale Research Letters* **9**, 23 (2014).
- <sup>13</sup>M. Wu, E. Luna, J. Puustinen, M. Guina, and A. Trampert, *Nanotechnology* **25**, 205605 (2014).
- <sup>14</sup>R. Butkutė, K. Stašys, V. Pačebutas, B. Čechavičius, R. Kondrotas, A. Geižutis, and A. Krotkus, *Optical and Quantum Electronics* **47**, 873 (2015).
- <sup>15</sup>A. Arnoult and J. Colin, Patent FR1754616 (24 May 2017).
- <sup>16</sup>S. M. Newstead, A.A. Kubiak, E.H.C. Parker, *Journal of Crystal Growth* **81**, 49 (1987).
- <sup>17</sup>M.R. Fahy, X.M. Zhang, E.S. Tok, J.H. Neave, P. Vaccaro, K. Fujita, M. Takahashi, T. Watanabe, K. Sato, B.A. Joyce, *Thin Solid Films* **306**, 192 (1997).
- <sup>18</sup>H. Makhloufi, P. Boonpeng, S. Mazzucato, J. Nicolai, A. Arnoult, T. Hungria, G. Lacoste, C. Gatel, A. Ponchet, H. Carrere, X. Marie, and C. Fontaine, *Nanoscale Research Letters* **9**, 123 (2014).
- <sup>19</sup>G. G. Stoney, *Proceedings of the Royal Society A: Mathematical, Physical and Engineering Sciences* **82**, 172 (1909).
- <sup>20</sup>J.C. Brice, INSPEC, EMIS Datareviews Series n°2 (1986), ISBN 0 85296 323 8.
- <sup>21</sup>J. J. Colin, G. Abadias, A. Michel, and C. Jaouen, *Acta Materialia* **126**, 481(2017).
- <sup>22</sup>S. Tixier, M. Adamcyk, and T. Tiedje, S. Francoeur, A. Mascarenhas, Peng Wei and F. Schiettekatte, *Appl. Phys. Lett.* **82** (14), 2245 (2003).
- <sup>23</sup>F. Brunner, A. Knauer, T. Schenk, M. Weyers, and J. -T. Zettler, *Journal of Crystal Growth* **310**, 2432 (2008).

- <sup>24</sup>R. France and A. J. Ptak, *J. Vac. Sci. Technol. B* **29** (3) 03C115-1 (2011).
- <sup>25</sup>R. France, a C.-S. Jiang, and A. J. Ptak, *Applied Physics letters* **98**, 101908 (2011).
- <sup>26</sup>X. Lu, B.A. Beaton, R.B. Lewis, T. Tiedje, and M.B. Whitwick, *Applied Physics letters* **92**, 192110 (2008).
- <sup>27</sup>J. -M. Gerard and G. Le Roux, *Applied Physics Letters* **62**, 3452 (1993).
- <sup>28</sup>R. Kaspi and K. Evans , *Journal of Crystal Growth* **175**, 838 (1997).
- <sup>30</sup>A. Duzik, J. C. Thomas, A. van der Ven, and J. M. Millunchick, *Physical Review B* **87**, 035313 (2013).
- <sup>30</sup>P. Laukkanen, M. P. J. Punkkinen, H. -P. Komsa, M. Ahola-Tuomi, K. Kokko, M. Kuzmin, J. Adell, J. Sadowski, R. E. Perälä, M. Ropo, T. T. Rantala, I. J. Väyrynen, M. Pessa, L. Vitos, J. Kollár, S. Mirbt, and B. Johansson, *Physical Review Letters* **100**, 086101 (2008).
- <sup>31</sup>E. C. Young, S. Tixier, and T. Tiedje, *Journal of Crystal Growth* **279**, 316 (2005).
- <sup>32</sup>R. D. Richards, F. Bastiman, C. J. Hunter, D. F. Mendes, A. R. Mohmad, J. S. Roberts, and J. P. R. David, *Journal of Crystal Growth* **390**, 120 (2014).
- <sup>33</sup>D. F. Reyes, F. Bastiman, C. J. Hunter, D. L. Sales, A. M. Sanchez, J. P. R. David, and D. Gonzalez, *Nanoscale Research Letters* **9**, 23 (2014).
- <sup>34</sup>A. R. Mohmad, F. Bastiman, C. J. Hunter, F. Harun, D. F. Reyes, D. L. Sales, D. Gonzalez, R. D. Richards, J. P. R. David, and B. Y. Majlis, *Semicond. Sci. Technol.* **30**, 094018 (2015).